Journal of Molecular Structure 890 (2008) 272–276

Contents lists available at ScienceDirect

Journal of Molecular Structure

journal homepage: www.elsevier.com/locate/molstruc

Synthesis, structure and physical characterization of the dimer $\{[(bpy)_2Co]_2(TPOA)\}^{4+}$ (bpy = 2,2′-dipyridyl; H_2TPOA = *N*,*N*′,*N*″,*N*‴-tetraphenyl oxalamidine) ☆

Carlos Martí-Gastaldo [a], Zhi-Rong Qu [b], Sergio Tatay [a], Mario Ruben [b,*], Jose R. Galán-Mascarós [a,*]

[a] Instituto de Ciencia Molecular, Fundación General de la Universidad de Valencia y Universidad de Valencia, Polígono de la Coma, s/n, 46980 Paterna, Spain
[b] Institute of Nanotechnology, KIT, PF 3640, D-76021 Karlsruhe, Germany

ARTICLE INFO

Article history:
Received 30 January 2008
Received in revised form 1 May 2008
Accepted 7 May 2008
Available online 15 May 2008

Keywords:
Cobalt(III) complexes
Dimers
Oxalamidine
Synthesis and crystal structure

ABSTRACT

The reaction between $CoCl_2$, 2,2′-dipyridyl (bpy) and *N*,*N*′,*N*″,*N*‴-tetraphenyl oxalamidine (H_2TPOA) in a water/ethanol mixture yields the $\{[(bpy)_2Co]_2(TPOA)\}^{2+}$ dimer, that is immediately oxidized in aerobic conditions leading to the Co^{III} species $\{[(bpy)_2Co]_2(TPOA)\}^{4+}$. This cation was isolated as the $\{[(bpy)_2Co]_2(TPOA)\}(PF6)_4$ (**1**) salt, that was characterized by X-ray diffraction on single crystals. The dimer is formed by two Co^{III} ions in octahedral coordination bridged by a deprotonated μ_2-TPOA ligand. The Co^{III} ions appear in its low spin configuration. Thus, the dimers are essentially diamagnetic, as shown by ^1H NMR and magnetic measurements.

1. Introduction

The field of molecule-based magnets has experienced a rapid and continuous growth since the discovery in the last decades that such materials could indeed compete with classic inorganic solids [1], while adding the intrinsic properties of molecules, offering incomparable possibilities for the design of tailor-made new materials.

In a general approach, molecule-based magnets are obtained by combination of paramagnetic metal centers, as spin carriers, with organic ligands acting as bridges and responsible for the appearance of magnetic exchange, that can give rise to the magnetically ordered phase. Room temperature magnets [2], organic magnets [3], hard magnets [4], photo-active magnets [5], conducting magnets [6], chiral magnets [7] or soluble magnets [8] are among the most remarkable achievements obtained with this strategy. However, all these examples have been prepared from few ligands, only those capable of mediating sufficiently strong magnetic interactions between metal ions such that bulk magnetic ordering can occur. Apart from monoatomic ligands (as oxide or halide), only cyanide, dicyanamide, oxalate or analogous ligands have shown to be able to promote strong enough magnetic superexchange to be useful in the design and preparation of molecule-based materials. All these ligands have in common that the exchange pathway is three atoms long or shorter, and all of them offer a σ and a π pathways. Longer bridges only offer interesting results, from the magnetic point of view, when the ligand is also a spin carrier, i.e., organic radical [9].

In our quest for new ligand systems to be incorporated into the design of new molecule-based magnets in order to achieve improved magnetic exchange properties, we decided to investigate further the oxalate motif; one of the most frequently used ligand systems (Scheme 1). Theoretical studies [10] have indeed predicted, using semiempirical Hückel theory methods, that among the oxalate family of ligands, progressive substitution of oxygen by less electronegative donor atoms (e.g., S or N) should increase the magnitude of the antiferromagnetic (AF) exchange. According to these theoretical predictions, the all-sulfur substituted oxalate analog, the tetrathiooxalate, should provide the highest magnetic coupling strength. But it was shown that this class of ligands suffers from the serious drawback of coordination instability against most of the paramagnetic d-metals [11]. Going for all nitrogen substitution seems to be a good compromise between increased magnetic exchange properties and reliable coordination chemistry, since the resulting ligands should behave similar to the known class of diazadiene exhibiting high degree of σ-bonding and π-backbonding. However, it was shown that the aromatic analogs, such as bipyrimidine or bisimidazole, do not considerably promote

☆ This paper is dedicated to the memory of Prof. Frank Albert Cotton, a constant and living inspiration for all chemists, scientists and scholars.

* Corresponding authors. Tel.: +34 963544420; fax: +34 963543273.
E-mail addresses: Mario.Ruben@int.fzk.de (M. Ruben), jose.r.galan@uv.es (J.R. Galán-Mascarós).

0022-2860/$ - see front matter © 2008 Elsevier B.V. All rights reserved.
doi:10.1016/j.molstruc.2008.05.011

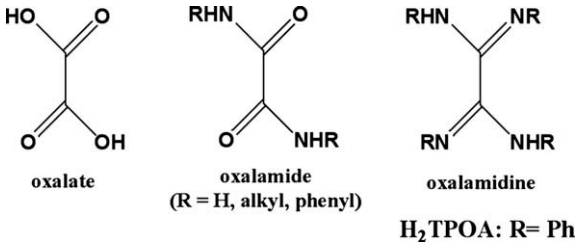

Scheme 1.

magnetic superexchange [12]. On the other hand, the partially substituted non-aromatic oxalamides have been proven to be a valuable bridging ligand in a multitude of magnetically coupled systems (Scheme 1) [13]. The all-nitrogen substituted oxalates, the oxalamidines, combine strong magnetic interactions with excellent coordination stability against open spin d-metal ions. Oxalamidines have been used extensively as ligands in Ru^{II}-based polypyridyl dyes [14], in catalysts to oligomerize and to polymerize ethylene [15] or as its Mg^{II} carbamato-complexes in CO_2-fixation and -activation reactions mimicking the pivotal Ribulose-1,5-biphosphatecarboxylase/oxygenase (RUBISCO) enzyme in the dark cycle of the natural photosynthesis [16]. More recently, the reductive coupling of carbodimides with metallic lithium leading to coordinated oxalamidino complexes was reported. Here, we report our results in the attempt to prepare and characterize an octahedral Co^{II} dimer with one bridging oxalamidine, the *N*,*N*′,*N*″,*N*‴-tetraphenyl oxalamidine (H_2TPOA).

2. Experimental

2.1. Synthesis

All reagents were obtained from commercial sources and used without further purification. The ligand H_2TPOA was prepared following a standard literature procedure [17]. ^{1}H NMR (300 MHz, DMSO-d_6): δ 9.82 (s, 2H), 7.80 (d, J = 7.8 Hz, 4H), 7.27 (t, J = 7.8 Hz, 4H), 7.08 (t, J = 7.6 Hz, 4H), 6.98 (t, J = 7.3 Hz, 4H), 6.89 (t, J = 7.3 Hz, 4H), 6.49 (d, J = 7.6 Hz, 4H).

2.1.1. Preparation of {[(bpy)$_2$Co]$_2$(TPOA)}[PF$_6$]$_4$ (**1**)

$CoCl_2{\cdot}4H_2O$ (0.2 mmol; 0.046 g), 2,2′-bipyridyl (0.4 mmol; 0.062 g) and H_2TPOA (0.1 mmol; 0.039 g) were dissolved in 10 mL of absolute EtOH with continuous stirring up to 15 min, leading to an orange solution. An excess of $NaPF_6$ (2 mmol; 0.336 g) was dissolved in 5 mL of water. The ethanolic solution was layered carefully onto the aqueous solution in a small diameter glass tube. After 4 days, brown square shaped crystals were filtrated, washed thoroughly with water and dried in air; yield (34%). ^{1}H NMR (300 MHz, DMSO-d_6): δ 9.21 (d, J = 5.5 Hz, 4H$_{py1}$), 8.88 (t, J = 7.7 Hz, 4H$_{py1}$), 8.69 (d, J = 7.7 Hz, 4H$_{py1}$), 8.62 (t, J = 6.6 Hz, 4H $_{py1}$), 8.15 (d, J = 7.9 Hz, 4H$_{py2}$), 7.93 (t, J = 7.6 Hz, 4H$_{py2}$), 7.28 (t, J = 6.3 Hz, 4H$_{py2}$), 7.15 (d, J = 5.5 Hz, 4H$_{py2}$), 6.56 (t, J = 7.3 Hz, 4H$_{TPOA}$), 6.36 (t, J = 7.9 Hz, 4H$_{TPOA}$), 6.30 (d, J = 8.2 Hz, 4H$_{TPOA}$), 6.22 (t, J = 7.5 Hz, 4H$_{TPOA}$), 5.70 (d, J = 7.8 Hz, 4H$_{TPOA}$). IR (cm^{-1}): 3590, 3306 (m, N—H stretching); 1640 (m, C=N stretching); 1608, 1597 (s, arom. C=C stretching);); 1448 (s, C=C); 1245 (w–m, arom. in-plane C—H 844, 561 (vs, PF_6^-); 764, 700 (s, arom. out-of-plane = C—H).

2.2. X-ray crystallography

A single crystal of **1** was secured on a glass fiber and mounted on a Kappa CCD Smart X-ray diffractometer equipped with graphite-monochromated MoKα radiation (λ = 0.71073 Å). All frames were collected at room temperature, and corrected for absorption using the Kappa CCD software package (MAXUS) [18]. The structure was solved by direct methods using the SIR97 program [19] and refined on F^2 with the SHELXL-97 program [20]. Cell parameters and crystallographic data are given in Table 1. The PF_6^- anions appear heavily disordered. The F atoms were fitted to a disordered model, with occupancy factors lower than one and restrained distance parameters. This disorder did not affect any of the positions from the complexes, but it contributed to the high R values obtained. Only heavy atoms (Co and P) and the N atoms directly linked to the metals could be refined anisotropically. All H atoms were located in their calculated positions, and assigned a thermal factor 20% larger than that of the atoms they are linked to. Additional calculations were performed with the PLATON software [21], and showed that no solvent accessible void was found. All crystallographic representations were generated with the CrystalMaker software package.

2.3. Equipment

Solution 1H NMR spectra were recorded on a Brucker Avance DRX spectrometer at 300 MHz. Infrared spectra were recorded in a FT-IR Nicolet 5700 spectrometer (4000–400 cm^{-1} range) using powdered samples in KBr pellets. Magnetic susceptibility measurements were performed on a polycrystalline sample with a Quantum Design MPMS-XL5 susceptometer equipped with a SQUID sensor. Susceptibility data were corrected from the diamagnetic contributions as deduced by using Pascal's constant tables. DC data were collected in the 2–300 K range under an applied field of 1000 G.

3. Results and discussion

The salt {[(bpy)$_2$Co]$_2$(TPOA)}[PF$_6$]$_4$ (**1**) was prepared by slow diffusion of an ethanolic solution of $CoCl_2{\cdot}4H_2O$, 2,2′-bipyridyl and H_2TPOA into an aqueous solution of $NaPF_6$. All our attempts to crystallize in good yield the corresponding Co^{II} salt {[(bpy)$_2$-

Table 1
Crystal data and structure refinement parameters for {[(bpy)$_2$Co]$_2$(TPOA)}[PF$_6$]$_4$ (**1**).

Empirical formula	$C_{66}H_{52}Co_2F_{24}N_{12}P_4$
Formula weight	1710.94
Temperature (K)	293(2)
Wavelength (Å)	0.71073
Crystal system, space group	Orthorhombic, P*na2$_1$*
Unit cell dimensions	
a (Å)	24.4800(9)
b (Å)	14.1750(12)
b (Å)	19.849(2)
Volume (Å$_3$)	6887.7(10)
Z	4
Absorption coefficient (mm^{-1})	0.692
F(000)	3448
Crystal size (mm^3)	0.42 × 0.24 × 0.22
θ Range	2.43–21.95°
Limiting indices	$-25 \leqslant h \leqslant 25$, $-14 \leqslant k \leqslant 14$, $-20 \leqslant l \leqslant 20$
Completeness to maximum θ	94.1%
Reflections collected/unique	7126/3389
Refinement method	Full-matrix least-squares on F^2
Data/restraints/parameters	3389/45/448
Goodness-of-fit on F^2	0.968
Final R indices [$I > 2\sigma(I)$][a,b]	R_1 = 0.0953, wR_2 = 0.1991
R indices (all data)	R_1 = 0.2149, wR_2 = 0.2684
Largest diff. peak and hole	0.599 and −0.475 e Å^{-3}

[a] $R_1 = \Sigma\, ||F_O|-|F_C||/\, \Sigma\, |F_O|$.

[b] $wR_2 = \left\{\sum \left[w(F_O^2 - F_C^2)^2\right] / \sum \left[w(F_O^2)_2\right]\right\}^{1/2}$; where $w = [\sigma_2(F_O^2) + (0.1228P)^2]^{-1}$ and $P = (F_O^2 + 2F_C^2)/3$.

$Co]_2(TPOA)\}[PF_6]_2$ failed. Direct reaction gives not a pure compound, and crystallization in inert atmosphere didn't yield any crystalline material in the conditions we tried. The stability of the reagents in air, where Co^{II} remains in solution for days or weeks, clearly indicates that the Co^{II} centers are oxidized by air (or other agents) only when the dimer is formed. As it is well known, ligands that favor strong crystal field also stabilize the Co^{III} and this shows that the selection of bpy as the terminal ligands was not a good choice for the purpose of generating a magnetic Co^{II} dimer.

1 crystallizes in the *Pna2₁* orthorhombic space group and contains the $\{[(bpy)_2Co]_2(TPOA)\}^{4+}$ dimer (Fig. 1), formed by two octahedral Co centers bridged together by a μ_2-TPOA bis-chelating bridge. The Co centers were determined to be Co^{III} species. This was suggested by the metal to ligand distances, since all Co–N distances appear in the 1.90–1.95 Å range, typical of low spin Co^{III}, whereas Co^{II} would present bonding distances well over 2.00 Å (Table 2). In addition, the CoN_6 geometry fits a perfect octahedral distribution, with very small deviations from orthogonality, due to the bite angle of the ligands for bpy and TPOA (N—Co—N angle = 82° and 83°, respectively. In order to confirm this extent, NMR measurements for **1** were performed. The ^1H NMR spectra showed the typical pattern for the deprotonated ligand, with all signals appearing at typical fields, ruling out the presence of paramagnetic Co^{II} centers [22]. Paramagnetic centers would give rise to relevant paramagnetic relaxation in the spectra.

According to the number of anions present the μ_2-TPOA ligand is supposed to be unprotonated, although the bonding C—N distances (C1—N4 = 1.28(2) Å) are slightly shorter than those reported for bridging deprotonated TPOA, where all C—N distances are in the range of 1.32–1.34 Å [23]. The metal centers complete their coordination sphere with two 2,2′-dipyridyl ligands each. No significant distortions from regular octahedral are observed.

Probably due to the bulky phenyl rings of the H_2TPOA ligand, the Co^{III} centers are forced to adopt the same chirality in each given dimer. A racemic mixture of both dimers, ΛΛ and ΔΔ, is present in the crystal structure (with a Flack parameter close to ½). The space group is achiral, although also acentric. The dimers pack forming layers parallel to the *ab* plane, with a pseudo-hexagonal array, where each dimer is surrounded by four dimers of opposite chirality (Fig. 2), and two dimers of the same chirality along the *a* axis. The anions occupy the holes in the interlayer space, and appear heavily disordered with respect to the orientation of the fluorine atoms. The overall +4 charge for the dimer is neutralized by the presence of four PF_6^-) anions per dimer in the unit cell.

Table 2
Selected bond distances and angles for $\{[(bpy)_2Co]_2(TPOA)\}[PF_6]_4$ (**1**)

Co1—N8	1.916(15) Å
Co1—N1	1.918(13) Å
Co1—N5	1.930(14) Å
Co1—N6	1.927(15) Å
Co1—N7	1.949(15) Å
Co1—N2	1.936(12) Å
Co2—N10	1.926(13) Å
Co2—N12	1.932(15) Å
Co2—N4	1.966(13) Å
Co2—N3	1.969(12) Å
Co2—N9	1.970(15) Å
Co2—N11	1.981(13) Å
N8—Co1—N1	177.4(6)°
N8—Co1—N5	88.3(6)°
N1—Co1—N5	94.2(6)°
N8—Co1—N6	94.0(6)°
N1—Co1—N6	87.2(6)°
N5—Co1—N6	84.5(6)°
N8—Co1—N7	83.3(6)°
N1—Co1—N7	95.7(6)°
N5—Co1—N7	92.4(6)°
N6—Co1—N7	176.0(6)°
N8—Co1—N2	95.3(6)°
N1—Co1—N2	82.2(5)°
N5—Co1—N2	176.3(6)°
N6—Co1—N2	96.1(6)°
N7—Co1—N2	87.1(6)°
N10—Co2—N12	93.4(6)°
N10—Co2—N4	93.3(5)°
N12—Co2—N4	95.0(6)°
N10—Co2—N3	175.4(6)°
N12—Co2—N3	90.1(6)°
N4—Co2—N3	83.5(5)°
N10—Co2—N9	82.6(6)°
N12—Co2—N9	174.1(5)°
N4—Co2—N9	89.7(6)°
N3—Co2—N9	94.1(6)°
N10—Co2—N11	89.4(5)°
N12—Co2—N11	84.3(6)°
N4—Co2—N11	177.3(5)°
N3—Co2—N11	93.9(5)°
N9—Co2—N11	91.2(6)°

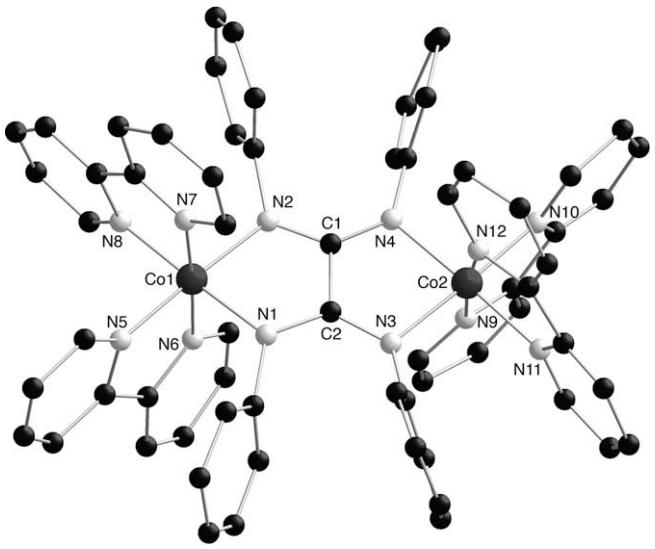

Fig. 1. Representation of the molecular structure for the $\{[(bpy)_2Co]_2(TPOA)\}^{4+}$ dimers in **1**.

Magnetic data were collected in grained single crystals of the title compound (Fig. 3). A paramagnetic signal was found with a very low magnetic moment at room temperature for $\chi_m T$ (1.07 emu K mol^{-1}). From this room temperature value the magnetic moment decreases monotonically as the temperature is decreased. This behavior is typical of a temperature independent paramagnetism ($\chi_{TIP} = 2 \times 10^{-3}$ emu mol^{-1}) that dominates the high temperature regime. Below 50 K there is a subtle change in slope, and the decrease becomes slightly faster. The exponential behavior of χ_m at very low temperatures indicates that, since the ground state is diamagnetic for a low spin Co^{III} dimer, a paramagnetic impurity exists, probably coming from Co^{II} ions that were not oxidized during the crystallization randomly distributed in the dimmers. The data can be fitted to a simple model accounting for both contributions: $\chi_m T = \chi_{TIP} T + C\ T/(T - \theta)$, where C and θ are, respectively, the Curie and Weiss constants for the paramagnetic species. The value obtained for C suggests that approximately 8% of Co ions remain in the divalent high

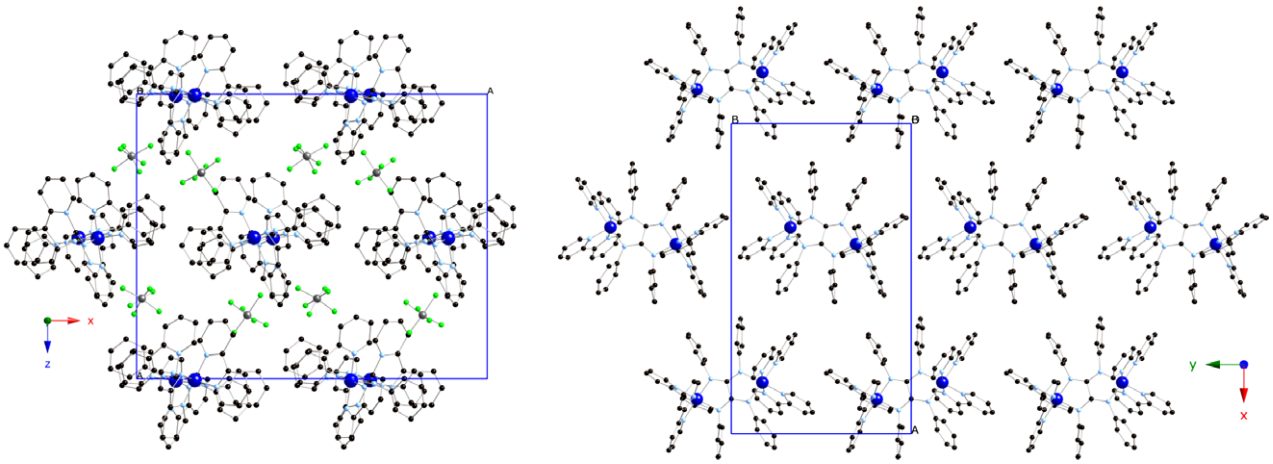

Fig. 2. Two views for the packing of the $\{[(bpy)_2Co]_2(TPOA)\}^{4+}$ dimers in $\{[(bpy)_2Co]_2(TPOA)\}[PF_6]_4$ (**1**): on the *ac* planes (left) and on the *ab* plane (right).

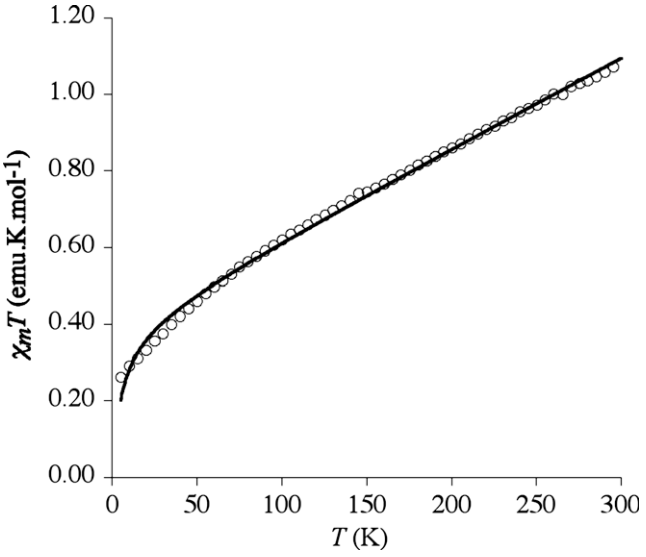

Fig. 3. Magnetic moment ($\chi_m T$ product) for the $\{[(bpy)_2Co]_2(TPOA)\}[PF_6]_4$ (**1**) salt in the 2–300 K (open circles), and magnetic fit for $C = 0.395$ emu K mol^{-1} ($\theta = -5$ K) and $\chi_{TIP} = 2 \times 10^{-3}$ emu mol^{-1}.

spin paramagnetic state. The χ_{TIP} is in good agreement with that expected for octahedral Co^{III} diamagnetic complexes, and arises from the distortion in the octahedral environment [24].

4. Summary

Although oxalamidines are theoretically good bridging ligands able to bridge paramagnetic d-metal ions for effectively providing strong magnetic coupling, our results show that more elements need to be taken into account for successfully building magnetic compounds with transition metal ions. The possibility to favor low spin states in the metal centers must be carefully controlled at the time to select terminal ligands to stabilize the corresponding dimers or oligomers. High crystal field ligands, such as bipyridines, in an octahedral environment with oxalamidines produce strong ligand field. In the case of Co^{II}, this favors low spin states and it finally promotes metal oxidation by air. All our attempts to isolate these dimers in anaerobic conditions to avoid metal oxidation did not yield crystalline products. We have also found out that analogous dimers with other redox stable metals, as Ni^{II}, cannot be easily isolated, and all our attempts were not successful. We also performed multiple tests with other anions with different shapes (ClO_4^-), Cl^-, SO_4^{2-})) but for the moment it is clear that the $\{[(bpy)_2M]_2(TPOA)\}^{4+}$ species are a much easier to crystallize in the reaction conditions we described that the corresponding $\{[(bpy)_2M]_2(TPOA)\}^{2+}$ analogs, no matter the metals used in this case. Substitution of bpy for other ligands, such as acetylacetonate, did not yield better results in these cases. The possibility to build dimers based on tetrahedral metals [22], always in their high spin state, could also solve the present problem. Further work in these directions is in progress.

Acknowledgements

The authors thank the ERANET-Chemistry program of the National Funding Agencies for financial support within the frame of the project "MULTIFUN". This work was supported by the Spanish Ministerio de Educación y Ciencia (CTQ2005-25211 and CTQ2006-27186 and CSD2007-00010 Consolider-Ingenio project in Molecular Nanoscience) and by the Generalitat Valenciana (ACOMP07/074). C.M.G. and S.T. thank the MEC for a Ph.D. grant.

Appendix A. Supplementary data

Supplementary data associated with this article can be found, in the online version, at doi:10.1016/j.molstruc.2008.05.011.

References

[1] E. Coronado, P. Delhaès, D. Gatteschi, Molecular Magnetism: From Molecular Assemblies to the Devices, in: J.S. Miller (Ed.), NATO ASI Series, vol. E321, 1996.
[2] T. Mallah, S. Thiebaut, M. Verdaguer, P. Veillet, Science 262 (1993) 1554;
J.M. Manriquez, G.T. Yee, R.S. McLean, A.J. Epstein, J.S. Miller, Science 252 (1991) 1415.
[3] J.S. Miller, A.J. Epstein, W.M. Reiff, Science 240 (1988) 40.
[4] M. Kurmoo, C.J. Kepert, New J. Chem. 22 (1998) 1515;
J.L. Manson, C.R. Kmety, Q.Z. Huang, J.W. Lynn, G.M. Bendele, S. Pagola, P.W. Stephens, L.M. Liable-Sands, A.L. Rheingold, A.J. Epstein, J.S. Miller, Chem. Mater. 10 (1998) 2552.
[5] O. Sato, T. Iyoda, A. Fujishima, K. Hashimoto, Science 272 (1996) 704.
[6] E. Coronado, J.R. Galán-Mascarós, C.J. Gómez-García, V. Laukhin, Nature 408 (2000) 447.
[7] E. Coronado, J.R. Galán-Mascarós, C.J. Gómez-García, A. Murcia-Martínez, Chem. Eur. J. 12 (2006) 3484;
M. Minguet, D. Luneau, E. Lhotel, V. Villar, C. Paulsen, D.B. Amabilino, J. Veciana, Angew. Chem. Int. Ed. 41 (2002) 586;
K. Inoue, H. Imai, P.S. Ghalsasi, K. Kikuchi, M. Ohba, H. Okawa, J.V. Yakhmi, Angew. Chem. Int. Ed. 40 (2001) 4242.
[8] E. Coronado, J.R. Galán-Mascarós, C. Martí-Gastaldo, Inorg. Chem. 46 (2007) 8108;

E. Coronado, J.R. Galán-Mascarós, C. Martí-Gastaldo, Inorg. Chem. 45 (2006) 1882.
[9] J.-H. Her, P.W. Stephens, K.I. Pokhodnya, M. Bonner, J. Miller, Angew. Chem. Int. Ed. 119 (2007) 1543.
[10] R. Vicente, J. Ribas, S. Alvarez, A. Seguí, X. Solans, M. Verdaguer, Inorg. Chem. 26 (1987) 4004.
[11] R. Vicente, J. Ribas, S. Alavarez, A. Segui, X. Solans, M. Verdaguer, Inorg. Chem. 26 (1987) 4004.
[12] J. Cano, E. Ruiz, P. Alemany, F. Lloret, S. Alvarez, J. Chem. Soc., Dalton Trans. (1999) 1669.
[13] Some representative examples Y. Journaux, J. Sletten, O. Kahn, Inorg. Chem. 24 (1985) 4063;
J.A. Real, M. Mollar, R. Ruiz, J. Faus, F. Lloret, M. Julve, M. Philoche-Levisalles, J. Chem. Soc., Dalton Trans. (1993) 1483;
A. Cornia, A.C. Fabretti, F. Ferraro, D. Gatteschi, A. Gusti, J. Chem. Soc., Dalton Trans. (1993) 3363.
[14] M. Ruben, A. Skirl, S. Rau, K. Krause, H. Görls, D. Walther, J.G. Vos, Inorg. Chim. Acta (2000) 206.
[15] D. Walther, M. Döhler, N. Theyssen, H. Görls, Eur. J. Inorg. Chem. 8 (2001) 2049.
[16] M. Ruben, D. Walther, R. Knake, H. Görls, R. Beckert, Eur. J. Inorg. Chem. 7 (2000) 1055;
D. Walther, M. Ruben, S. Rau, Coord. Chem. Rev. 182 (1999) 67.
[17] K. Bauer, Chem. Ber. 40 (1907) 2655.
[18] S. Mackay, C.J. Gilmore, M. Treymane, N. Stewart, K. Shankland, Maxus: A Computer Program for Solution and Refinement of Crystal Structure from Diffraction Data, University of Glasgow, Scotland, UK; Nonius BV, Delft, The Netherlands; MacScience Co. Ltd., Yokoama, Japan, 1999.
[19] A. Altomare, G. Cascarano, C. Giacovazzo, A. Guagliardi, M.C. Burla, G. Polidori, M. Camalli, J. Appl. Crystallogr. 27 (1994) 435.
[20] G.M. Sheldrick, University of Göttingen, 1997.
[21] A.L. Spek, Acta Crystallogr. A46 (1990) C34.
[22] M. Kita, H. Tamai, F. Ueta, A. Fuyuhiro, K. Yamanari, K. Nakajima, M. Kojima, K. Murata, S. Yamashita, Inorg. Chim. Acta 314 (2001) 139.
[23] M. Ruben, D. Walther, R. Knake, H. Görls, R. Beckert, Eur. J. Inorg. Chem. 7 (2000) 1055.
[24] J.S. Griffith, L.E. Orgel, Trans. Faraday Soc. 53 (1957) 601.